

Resource Allocation for Cognitive Radio-Enabled Femtocell Networks With Imperfect Spectrum Sensing and Channel Uncertainty

Yujie Zhang and Shaowei Wang, *Senior Member, IEEE*

Abstract—Deploying femtocells underlying macrocells is a promising way to improve the capacity and enhance the coverage of cellular systems. However, such a two-tier network also gives rise to a cross-tier and intratier interference issue that should be properly addressed to acquire the potential performance gain. In this paper, we study the resource-allocation (RA) problem in a two-tier orthogonal frequency-division multiplexing (OFDM) access-based heterogeneous cellular network, where the femtocells that employ a closed access strategy are equipped with a cognitive radio (CR) function to identify radio environment so that they can share subchannels with the macrocells without generating excessive interference to the macrocell users (MUs), which fall into the coverage of the femtocells. We formulate an optimization task to maximize the sum throughput of the femtocell users (FUs) under the consideration of imperfect spectrum sensing and channel uncertainty while controlling the interference to the MUs below their bearable thresholds in the sense of probability. We introduce a conservative convex approximation to the formulated problem and develop a fast algorithm to solve it by exploiting its structure. Simulation results show that our proposal can improve the throughput of the FUs with almost no changes in the infrastructure of the cellular network.

Index Terms—Chance-constrained optimization, cognitive radio (CR), resource allocation (RA), spectrum sensing.

I. INTRODUCTION

RECENT investigations have indicated that 50% of phone calls and 70% of wireless data services will take place in indoor environments in the coming decade [1]. Instead of increasing macrocells with high deployment cost to meet the exponentially increasing data demands, a user-installed femtocell access point (FAP) with a lower transmission power

Manuscript received May 18, 2015; revised July 22, 2015 and September 1, 2015; accepted October 26, 2015. Date of publication November 17, 2015; date of current version September 15, 2016. This work was presented in part at the IEEE 2015 Wireless Communications and Networking Conference, New Orleans, LA, March 9–12, 2015. This work was supported in part by JiangsuSF under Grant BK20151389, by the Fundamental Research Funds for the Central Universities under Grant 021014380013, and by the Open Research Fund of the National Mobile Communications Research Laboratory under Grant 2016D08. The review of this paper was coordinated by Prof. Y. Qian. (*Corresponding author: Shaowei Wang.*)

Y. Zhang is with the School of Electronic Science and Engineering, Nanjing University, Nanjing 210023, China (e-mail: zhangyj@smail.nju.edu.cn).

S. Wang is with the School of Electronic Science and Engineering, Nanjing University, Nanjing 210023, China, and also with the National Mobile Communications Research Laboratory, Southeast University, Nanjing 210096, China (e-mail: wangsw@nju.edu.cn).

Color versions of one or more of the figures in this paper are available online at <http://ieeexplore.ieee.org>.

Digital Object Identifier 10.1109/TVT.2015.2500902

and lower cost, which usually serves a registered group of subscribers, is deemed as a promising solution to meeting the ever-increasing wireless data requirement [2]. Both users and operators can benefit from the deployment of the FAPs: Indoor users can enjoy high-quality-guaranteed wireless service, and outdoor users can acquire higher rate gains due to the FAPs; on the other hand, operators can cut down on operational expenditures since the traditional site survey and network planning process is no longer needed.

Generally, there are two modes for the FAPs to use the licensed spectrum of a cellular spectrum: One is to use a dedicated spectrum to avoid mutual interference between the femtocells and the macrocells; the other is to share all available spectra with the macrocells. The latter is more attractive since it has higher spectrum utilization efficiency [3]. However, a cross-tier interference issue rises as femtocell users (FUs) reuse the subchannels that have been already allocated to the macrocell users (MUs). In particular, for the MUs in the service area of an FAP, they may suffer heavy interference from the FAP because of their close proximity [4]. Moreover, perfect channel state information (CSI) is difficult to obtain in a practical cellular system owing to the lack of sufficient coordination between the FUs and the MUs, which further aggravates the interference among them. The cross-tier interference and intratier interference present challenges to the resource-allocation (RA) problem for the cellular network.

As for an orthogonal frequency-division multiplexing (OFDM) access-based femtocell network, RA is more complicated than that in a traditional OFDM system because the transmission power values of the femtocells and the macrocells differ from each other greatly, leading to awkward mutual interference between the two tiers. Power control [5], [6], multiple antennas [7], an adaptive FAP access scheme [8], [9], and spectrum allocation [10]–[12] have been extensively investigated to address the interference management problem in two-tier femtocell networks. In [8], a hybrid frequency assignment scheme is proposed for femtocells deployed within coverage of a macrocell to mitigate the cross-tier interference. In [13], power control is utilized to ensure adequate signal-to-interference-plus-noise ratio (SINR) for the indoor cell edge FU, and beamforming is used to maximize the SINR of MUs and FUs by mitigating cross-tier interference in a collaborative manner. A Stackelberg game with the macrocells as the leaders and the FAPs as the followers is modeled in [14], respectively. In the hierarchical competition, the performance of the system at Stackelberg equilibrium is proved to be much better than

that at Nash equilibrium. However, it is still very challenging to efficiently manage the random and severe interference resulting from numerous unplanned small cells.

Cognitive radio (CR), of which the original purpose is to improve the spectrum utilization efficiency, is also suggested as a promising interference management method for the problem RA in heterogeneous networks [15]. If the femtocells that share subchannels with the macrocells are equipped with a CR function, they can identify the radio environment of the cellular system and choose to access the subchannels that can produce the least interference to the MUs. Since the physical layer of a CR system should be very flexible to meet the requirements of opportunistic access, it is necessary to use multicarrier methods to operate in CR networks. Owing to the inherent significant advantages of flexibly allocating radio resource, OFDM is deemed as a promising air interface for Long-Term Evolution (LTE) femtocells [16]. With OFDM modulation, the intratier interference can be eliminated by exploiting orthogonal radio resources among femtocells. Thus, an important issue that follows is how to effectively assign orthogonal radio resources between macrocells and femtocells while considering cross-tier interference, which is the motivation of this paper.

The RA problem in the CR-based femtocell networks has been investigated in the literature. In [17] and [18], downlink RA problems based on spectrum sharing between macrocells and femtocells are studied, including a decentralized femtocell self-regulation strategy for the FAPs to adjust their transmit power values [17] and design and analysis underlay spectrum sharing schemes [18]. In [19], an efficient algorithm is proposed for the open access scenario to improve the throughput of cognitive femtocell networks. Game-theoretic RA in cognitive femtocell networks is investigated in [20] with correlated equilibrium analysis. In [21], two cooperation models are proposed for the FUs and MUs in a cognitive femtocell network. In these studies, perfect CSI is assumed. However, wireless channel is generally time varying. The users will go through severe quality-of-service (QoS) degradation and even outage if unfaithful CSI is used to design the transmission without considering channel uncertainty. Therefore, RA schemes considering channel uncertainty should be studied for the CR-based femtocell networks.

In [22], a power-allocation problem that characterizes robustness and energy efficiency in femtocell networks is considered, for which a distributed algorithm, i.e., a standard interference function algorithm, is introduced when taking uncertain gains into consideration. In [23], the focus is on the transmit beamforming design for femtocells under QoS constraints and imperfect CSI. An efficient interior-point-based algorithm is proposed to find the optimal beamforming design. In [24], a class of RA problems is formulated, where the quality-of-experience model and playout time of the multimedia applications are unknown to the controller. Dynamic RA schemes are proposed to achieve a satisfying tradeoff between the test and optimization. Distributed wireless video scheduling with delayed control information is investigated in [25], where a class of distributed scheduling schemes is proposed to achieve the performance bound by using the correlation among the timescale control information.

In addition, owing to the inherent feedback delays, sensing errors, which include estimation errors and quantization errors, are inevitable, causing heavy interference to the MUs. To avoid performance degradation of the MUs, RA with imperfect spectrum sensing should be also urgently considered. However, to the best of our knowledge, RA considering both channel uncertainty and imperfect sensing in OFDM-based cognitive femtocell networks has not been extensively investigated in existing studies.

In this paper, we put the mutual interference, imperfect spectrum sensing, and channel uncertainty into consideration in two-tier OFDM-based cognitive femtocell networks. To the best of our knowledge, there are no existing works in the OFDM-based cognitive femtocell networks, which jointly take all these design issues into consideration. We try to maximize the sum throughput of all FUs under the condition of imperfect spectrum sensing while controlling the interference to the MUs under their bearable thresholds in the sense of probability due to imperfect CSI. These considerations lead to a general formulation of a mixed integer programming problem, which is computationally intractable. To make it tractable, we propose addressing this problem in three steps. In the first step, we try to allocate subchannels based on channel gains. For the second step, the interference constraints, which are posed as chance constraints due to channel uncertainty, are made tractable by the Bernstein approximation. For the third step, we try to allocate power to the subchannels. We propose a method by exploiting the structure of the problem, which is able to achieve the optimal power allocation and is much more efficient than standard methods. Numerical results validate the effectiveness and efficiency of our proposal.

The remainder of this paper is organized as follows. In Section II, we show the system model and formulate our optimization task. In Section III, we propose a suboptimal subchannel allocation algorithm and achieve an optimal power-allocation scheme by developing an efficient fast method with chance-constrained optimization. Numerical results are given in Section IV with discussions. Conclusions and future work are presented in Section V.

II. SYSTEM MODEL AND PROBLEM FORMULATION

Consider the downlink of a two-tier heterogeneous network, where M CR-equipped femtocells share the licensed radio spectrum with one macrocell. Each femtocell is served by an FAP, and the macrocell is served by a macro base station. The CR-based femtocell adopts OFDM modulation and operates in a centralized manner, i.e., an access point serves all FUs attached to it. We denote the set of all FUs associated with FAP $m \in \mathcal{M}$ as \mathcal{K}_m , and then, the number of FUs laid within the coverage of the m th FAP is $K_m = |\mathcal{K}_m|$. Let L and K denote the numbers of MUs and FUs, respectively. The FUs opportunistically use the spectrum of the MUs via an FAP, as shown in Fig. 1.

Any part of the spectrum, named as a subband, can be used by the MU at any time. The bandwidth is divided into multiple OFDM subchannels in the CR network. By periodic spectrum sensing, the CR network identifies vacant subchannels and

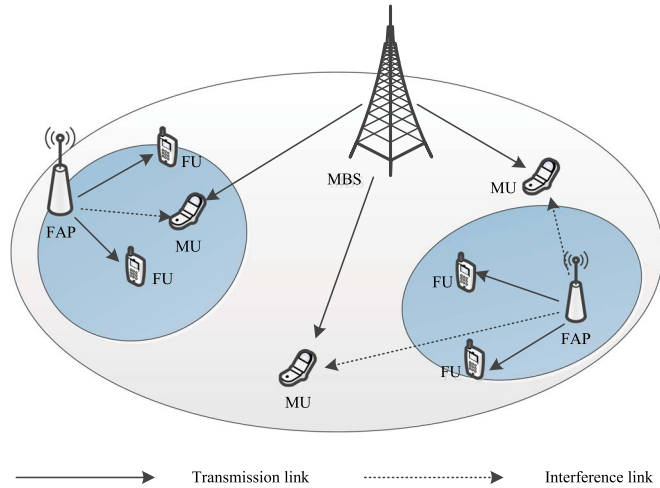


Fig. 1. Two-tier CR-based wireless heterogeneous network consisting of one macrocell and two femtocells.

chooses a subset $\mathcal{N} = \{1, \dots, N\}$ among all subchannels to transmit information. In addition, the k th FU has a minimal rate requirement of $R_{k,\min}$.

To prohibit the unacceptable performance degradation of the MUs, the interference introduced to the MUs must be carefully controlled in a tolerable range. Some promising methods can be employed by the CR system to eliminate the interference to the MUs, such as the subcarrier weighting and noncontinuous OFDM scheme. In this paper, we consider a general OFDM system that may not adopt noncontinuous OFDM or subcarrier weighting techniques. The total available bandwidth of the system is W . The bandwidth of the n th subchannel spans from $f_0 + (n-1)W/N$ to $f_0 + nW/N$, where f_0 is the starting frequency. When the femtocell transmits information over the n th subchannel with unit transmission power, the interference introduced to the l th MU over the subband of the j th subchannel is given by

$$I_{n,l}^j = \int_{(j-1)W/N - (n-1/2)\frac{W}{N}}^{jW/N - (n-1/2)\frac{W}{N}} g_{n,l} \phi_n(f) df \quad (1)$$

where $\phi_n(f)$ is the power spectrum density (PSD) of the subchannel used by an FU, which can be expressed as $\phi_n(f) = T_s (\sin \pi f T_s / \pi f T_s)^2$, where T_s is the OFDM symbol duration. $g_{n,l}$ is the power gain from the femtocell to the l th MU's receiver on the n th subchannel. Due to the absence of cooperation between the macrocell and the femtocells, it is difficult to obtain $g_{n,l}$. In other words, perfect CSI is always not available. To capture the channel uncertainty, $g_{n,l}$ is modeled as an exponentially distributed random variable [26].

There are two kinds of sensing errors [27], [28]. One is *misdetction*, which happens when the CR system fails to detect the presence of the MUs' signals. A subchannel is deemed as vacant, but it is actually occupied by the MUs. This may incur service degradation on the MUs. The other kind of sensing errors is *false alarm*, which happens when the CR system identifies that a subchannel is occupied but it is actually vacant. A *false alarm* event does not incur performance degradation on the MUs but lowers the potential spectrum utilization.

TABLE I
PROBABILITIES OF IMPERFECT SPECTRUM SENSING

Actual state	Sensing Results	Probability
Active $S_{n,l}^1$	Occupied E_n^1	$P\{E_n^1 S_{n,l}^1\} = 1 - P_n^m$
Active $S_{n,l}^1$	Vacant E_n^2	$P\{E_n^2 S_{n,l}^1\} = P_n^m$
Idle $S_{n,l}^2$	Vacant E_n^2	$P\{E_n^2 S_{n,l}^2\} = 1 - P_n^f$
Idle $S_{n,l}^2$	Occupied E_n^1	$P\{E_n^1 S_{n,l}^2\} = P_n^f$

Obviously, *misdetction* results in cochannel interference to the MU, whereas *false alarm* lowers the utilization efficiency of the spectrum. Generally, the CR-based FAP collects the sensed information on all FUs and makes a decision on which subchannel can be used by the FUs. Then, the set of available subchannels \mathcal{N} is predicted, the same to the set of unavailable subchannels $\bar{\mathcal{N}}$. The probabilities of two kinds of sensing errors, i.e., *misdetction* and *false alarm*, on n th subchannel are P_n^m and P_n^f , respectively.

There are four possible scenarios for spectrum sensing for the l th MU, as shown in Table I. $S_{n,l}^1$ and $S_{n,l}^2$ are the events of the presence and absence of the l th MU's signal on the n th subchannel. E_n^1 and E_n^2 are events that the CR FAP deems the n th subchannel as vacant or not vacant by spectrum sensing. Denote $P_{n,l}^1$ as the probability that the n th subchannel is actually used by the l th MU when the CR FAP deems it as vacant. Thus, we have

$$\begin{aligned} P_{n,l}^1 &= P\{S_{n,l}^1 | E_n^1\} \\ &= \frac{P\{E_n^1 | S_{n,l}^1\} P\{S_{n,l}^1\}}{P\{E_n^1 | S_{n,l}^1\} P\{S_{n,l}^1\} + P\{E_n^1 | S_{n,l}^2\} P\{S_{n,l}^2\}} \\ &= \frac{(1 - P_n^m) P_n^l}{(1 - P_n^m) P_n^l + P_n^f (1 - P_n^l)} \end{aligned} \quad (2)$$

where P_n^l is the *a priori* probability that the band of the n th subchannel is used by the l th MU. Similarly, we can define $P_{n,l}^2$ as the probability that the n th subchannel is indeed vacant when the CR system identifies it as occupied. Thus, we have

$$\begin{aligned} P_{n,l}^2 &= P\{S_{n,l}^2 | E_n^2\} \\ &= \frac{P\{E_n^2 | S_{n,l}^2\} P\{S_{n,l}^2\}}{P\{E_n^2 | S_{n,l}^1\} P\{S_{n,l}^1\} + P\{E_n^2 | S_{n,l}^2\} P\{S_{n,l}^2\}} \\ &= \frac{(1 - P_n^f) (1 - P_n^l)}{P_n^m P_n^l + (1 - P_n^f) (1 - P_n^l)}. \end{aligned} \quad (3)$$

Taking the two kinds of sensing errors into consideration, the interference introduced to the l th MU by the access of an FU on the n th subchannel with unit transmission power is

$$I_{n,l} = \sum_{j \in \mathcal{N}_1} P_{j,l}^1 I_{n,l}^j + \sum_{j \in \mathcal{N}} P_{j,l}^2 I_{n,l}^j \quad (4)$$

Define the SINR of the k th FU in femtocell m on the n th subchannel as

$$H_{m,k,n} = \frac{|c_{m,k,n}|^2}{\Gamma(N_0 W/N + I)} \quad (5)$$

where $c_{m,k,n}$ is the channel gain of the k th FU in femtocell m over subchannel n , and N_0 is the PSD of additive white Gaussian noise. Γ is the signal-to-noise-ratio (SNR) gap and can be represented as $\Gamma = -(\ln(5BER)/1.5)$ for an uncoded multiple quadrature amplitude modulation with a specified bit error rate (BER) [29]. The interference caused by the MUs' signals is I , which can be regarded as noise and measured by the receivers of FUs.

It is notable that in (5), intratier interference between femtocells is deemed as part of the thermal noise due to the serious relatively low power of the FAPs and wall penetration loss [2]. This is particularly suitable for sparsely deployed femtocells in remote suburbs, where intratier interference between femtocells can be ignored in comparison with cross-tier interference.

In addition, the transmission rate of the k th FU in femtocell m on the n th subchannel is

$$r_{m,k,n} = (W/N) \log_2(1 + p_{m,k,n} H_{m,k,n}), \quad (6)$$

where $p_{m,k,n}$ is the k th FU's transmission power on the n th subchannel in femtocell m .

Our target is to maximize the sum rate of the FUs under the transmit power limitations and the MUs' interference constraints, which leads to the following chance-constrained optimization problem:

$$\begin{aligned} & \max_{p_{m,k,n}, \rho_{m,k,n}} \sum_{m \in \mathcal{M}} \sum_{k \in \mathcal{K}_m} \sum_{n \in \mathcal{N}} \rho_{m,k,n} r_{m,k,n} \\ \text{s.t. } & \text{C1: } \sum_{n \in \mathcal{N}} \rho_{m,k,n} r_{m,k,n} \geq R_{k,\min} \quad \forall m, k \in \mathcal{K}_m \\ & \text{C2: } \sum_{k \in \mathcal{K}_m} \sum_{n \in \mathcal{N}} \rho_{m,k,n} p_{m,k,n} \leq P_t \quad \forall m \\ & \text{C3: } P_r \left\{ \sum_{m \in \mathcal{M}} \sum_{k \in \mathcal{K}_m} \sum_{n \in \mathcal{N}} \rho_{m,k,n} p_{m,k,n} I_{n,l} \leq I_l^{th} \right\} \\ & \quad \geq 1 - \epsilon \quad \forall l \\ & \text{C4: } p_{m,k,n} \geq 0 \quad \forall m, k, n \\ & \text{C5: } \rho_{m,k,n} \in \{0, 1\} \quad \forall m, k, n \\ & \text{C6: } \sum_{k \in \mathcal{K}_m} \rho_{m,k,n} \leq 1 \quad \forall m, n \end{aligned} \quad (7)$$

where $R_{k,\min}$ is the minimal rate requirement of the k th FU. $\rho_{m,k,n}$ can only be either 1 or 0, indicating whether the band of n th subchannel is used by the k th FU in femtocell m or not; P_t is the power limit of a femtocell; and I_l^{th} is the interference power threshold of the l th MU.

C1 is the throughput requirements of the FUs. C2 is the transmission power constraints. To tackle channel uncertainty, CR interference constraints under channel uncertainty can be posed as chance constraints, and C3 is the interference constraints, which enforce that the interference power at the l th MU stays below I_l^{th} with the probability of no less than $1 - \epsilon$. Parameter ϵ can take any value from the interval $\epsilon \in [0, 1)$, denoting the desired upper bound on the probability that the interference threshold is exceeded. In a practical situation, perfect CSI cannot be accurately acquired; then, the probability approach is more reasonable than a set-bounded approach. The channel gain estimate is provided as a probabilistic distribution that specifies the mean and covariance of the gains. C4 is intuitive. C5 and C6 indicate that subchannels are not shared among FUs.

TABLE II
SUBCHANNEL ALLOCATION

Algorithm: Subchannel Allocation Algorithm

```

1 Initialization:
2  $\mathcal{N}_t = \mathcal{N}, \Omega_k = \emptyset, \forall k$ ;
3 Set  $R_k = 0$  for any  $1 \leq k \leq K$ ;
4 for all FUs
5   while  $\mathcal{N}_t \neq \emptyset$  and  $R_k < R_{k,\min}$  for any  $1 \leq k \leq K$ 
6     Find  $k^*$  satisfies  $R_{k^*} - R_{k^*,\min} \leq R_k - R_{k,\min}$ ;
7     For  $k^*$ , find  $n^*$  satisfies  $r_{m^*,k^*,n^*} \geq r_{m^*,k^*,n}, \forall n$ ;
8     Update  $R_{k^*} = R_{k^*} + \log(1 + p_{m^*,k^*,n^*} H_{m^*,k^*,n^*})$ ;
9     Update  $\Omega_{k^*} = \Omega_{k^*} \cup n^*, \mathcal{N}_t = \mathcal{N}_t \setminus \{n^*\}$ ;
10  endwhile
11 endfor

```

III. RESOURCE ALLOCATION IN FEMTOCELLS BY USING CHANCE-CONSTRAINED OPTIMIZATION

A. Subchannel Allocation

We propose a suboptimal approach to allocate subchannels to the FUs. The motivation of our algorithm is as follows. In an OFDM-based femtocell network, the subchannel with high SNR for an FU may also bring more interference to the MUs that use this subchannel. In other words, the traditional water-filling method is not appropriate for CR scenarios because interference constraints also lay an upper bound of transmission power for each subchannel. This is to say that the interference introduced to the MUs and the SNR of a subchannel should be jointly considered to calculate the rate of the subchannel. Our method measures the achievable rate of the n th subchannel used by the k th FU in femtocell m as follows [30], [31]

$$r_{m,k,n} = (W/N) \log_2(1 + p_{m,k,n} H_{m,k,n}), \quad (8)$$

where $p_{m,k,n}^{\max}$ is the maximum achievable power for the k th FU in femtocell m on the n th subchannel

$$p_{m,k,n}^{\max} = \min \left(P_t, \min_{l \in \mathcal{L}} \left(\frac{I_l^{th}}{I_{n,l}} \right) \right) \quad (9)$$

where $I_{n,l}$ is the interference introduced to the l th MU by the access of an FU on the n th subchannel, which is calculated by exponentially distributed random variable $g_{n,l}$. It is worth noting that $I_{n,l}$ is determinate after initialization.

Denote Ω_k as the subchannel set occupied by the k th FU. \mathcal{N}_t is the set of FUs that has not been assigned subchannels during each iteration t , and \emptyset is an empty set. We allocate the FUs' subchannels to meet their minimal rate requirements. The principle of our subchannel allocation algorithm for the FUs is that the FU whose current rate is the farthest away from the target one has the priority to get a subchannel among the available ones. The procedure stops until all FUs' rate requirements are satisfied. For simplicity, the power of a subchannel is provisionally set as $\min(P_t/N, \min_{l \in \mathcal{L}}(I_l^{th}/I_{n,l}))$ to meet the power and interference limitations continuously. The operational procedure of the proposed algorithm is described in Table II.

B. Power Allocation by Chance-Constrained Optimization

1) *Bernstein Approximation of Chance Constraints*: Once given the subchannel allocation of the FUs, the power-allocation problem can be rewritten as

$$\begin{aligned}
 & \max_{p_{m,k,n}} \sum_{m \in \mathcal{M}} \sum_{k \in \mathcal{K}_m} \sum_{n \in \Omega_k} r_{m,k,n} \\
 \text{s.t. } & \text{C1: } \sum_{n \in \Omega_k} r_{m,k,n} \geq R_{k,\min} \quad \forall m, k \in \mathcal{K}_m \\
 & \text{C2: } \sum_{k \in \mathcal{K}_m} \sum_{n \in \Omega_k} p_{m,k,n} \leq P_t \quad \forall m \\
 & \text{C3: } P_r \left\{ \sum_{m \in \mathcal{M}} \sum_{k \in \mathcal{K}_m} \sum_{n \in \Omega_k} p_{m,k,n} I_{n,l} \leq I_l^{th} \right\} \geq 1 - \epsilon \\
 & \quad \forall l \\
 & \text{C4: } p_{m,k,n} \geq 0 \quad \forall m, k, n.
 \end{aligned} \tag{10}$$

However, it is not intuitive to express C3 in closed form, making the optimization problem intractable. Our target is to construct the chance constraints' computationally tractable approximation. Under the assumption that the constraints are affine in the perturbations and the entries in the perturbation vector are independent-of-each-other random variables, we exploit the structure of chance constraints and build a large deviation-type approximation, referred to as Bernstein approximation, of the chance-constrained problem. This approximation is convex and efficiently tractable, which is of significantly practical merit. Note that C3 in problem (10) is still computationally intractable; hence, we make a convex approximation of C3. Bernstein approximations have been viewed as a useful class of approximation techniques for the chance constraints [32]. Consider a general case where chance constraint written in the following form:

$$P_r \left\{ f_0(\mathbf{p}) + \sum_{n \in \mathcal{N}} \eta_n f_n(\mathbf{p}) < 0 \right\} \geq 1 - \epsilon \tag{11}$$

where η_n are random variables, and \mathbf{p} is a deterministic parameter vector. In this paper, we have $\mathbf{p} \in \mathbf{R}^{MKN \times 1}$, $\mathbf{p} = (p_{1,1,1}, \dots, p_{1,1,N}, \dots, p_{1,K,N}, \dots, p_{M,K,N})^T$. For (11), for a given η_n distribution, the following assumptions should be satisfied.

- 1) $f_n(\mathbf{p})$ is the function of \mathbf{p} and is affine in $\mathbf{p} \quad \forall n = 0, 1, \dots, N$.
- 2) η_n 's are independent random variables, and their marginal distributions φ_n belong to compact convex sets of probability distributions.
- 3) φ_n is a shared bounded support of $[-1, 1]$ and $-1 \leq \eta_n \leq 1 \quad \forall n = 1, 2, \dots, N$.

Under these assumptions, the following constraint constitutes a conservative substitute:

$$\inf_{\lambda > 0} \left[f_0(\mathbf{p}) + \lambda \sum_{n \in \mathcal{N}} \Omega_n (\lambda^{-1} f_n(\mathbf{p})) + \lambda \log \left(\frac{1}{\epsilon} \right) \right] \leq 0 \tag{12}$$

where $\Omega_n(y) \triangleq \max_{\pi_n} \log(\int \exp(xy) d\pi_n(x))$. In addition, it is guaranteed that (12) is convex [26], [32]. The approximation is useful when $\Omega_n(y)$ can be evaluated efficiently. In general, one can consider an upper bound for $\Omega_n(y)$ given by

$$\Omega_n(y) \leq \max \mu_n^- y, \mu_n^+ y + \frac{\sigma_n^2}{2} y^2, \quad n = 1, 2, \dots, N \tag{13}$$

where μ_n^-, μ_n^+ with $\mu_n^- \leq \mu_n^+$ and σ_n are constants that rely on the given families of probability distributions. Some examples can be found in [33]. Substituting $\Omega_n(\cdot)$ in (12) with this upper bound and invoking the arithmetic-geometric inequality, we have

$$\begin{aligned}
 & f_0(\mathbf{p}) + \sum_{n \in \mathcal{N}} \max \mu_n^- f_n(\mathbf{p}), \mu_n^+ f_n(\mathbf{p}) \\
 & + \sqrt{2 \log \frac{1}{\epsilon}} \left(\sum_{n \in \mathcal{N}} \sigma_n^2 f_n(\mathbf{p})^2 \right)^{\frac{1}{2}} \leq 0 \quad \forall l \tag{14}
 \end{aligned}$$

as a convex conservative substitute for (11).

Due to the sensing errors and the absence of collaboration between femtocells and macrocell, the CSI is imperfect in practical scenarios. To capture this uncertainty, $g_{n,l}$, which is the power gain from the femtocell to the l th MU's receiver on the n th subchannel, is modeled as a random variable. As a result, $I_{n,l}$ that is calculated from $g_{n,l}$ is also a random variable of given distributions. Assume that the distributions of $I_{n,l}$ have been bounded supports $[a_{n,l}, b_{n,l}]$. Then, we introduce constants $\alpha_{n,l} \triangleq 1/2(b_{n,l} - a_{n,l})$ and $\beta_{n,l} \triangleq 1/2(b_{n,l} + a_{n,l})$ to normalize the supports to $[-1, 1]$, which means that $\alpha_{n,l} \eta_k + \beta_{n,l} \in [a_{n,l}, b_{n,l}]$. Denote $f_0(\mathbf{p}) = -I_l^{th} + \sum_{n=1}^N \beta_{n,l} p_{m,k,n}$ and $f_n(\mathbf{p}) = \alpha_{n,l} p_{m,k,n}$ for $n \in \mathcal{N}$, and then (11) is equivalent to C3 in (10). Thus, substituting $f_0(\mathbf{p})$ and $f_n(\mathbf{p})$ into (14), noting that $p_{m,k,n} \geq 0$, we have

$$\begin{aligned}
 & -I_l^{th} + \sum_{m \in \mathcal{M}} \sum_{k \in \mathcal{K}_m} \sum_{n \in \Omega_k} \beta_{n,l} p_{m,k,n} + \mu_{n,l}^+ \alpha_{n,l} p_{m,k,n} \\
 & + \sqrt{2 \log \frac{1}{\epsilon}} \left(\sum_{k \in \mathcal{K}_m} \sum_{n \in \Omega_k} (\sigma_{n,l} \alpha_{n,l} p_{m,k,n})^2 \right)^{\frac{1}{2}} \leq 0 \quad \forall l. \tag{15}
 \end{aligned}$$

In fact, as the variables $p_{m,k,n}$'s are coupled through the last term in (15), the search complexity rapidly grows as N increases. To mitigate these issues, we further approximate (15) by noting that the last term in (15) involves the ℓ_2 -norm of the vector $[\sigma_{1,l} \alpha_{1,l} p_{m,k,1}, \dots, \sigma_{N,l} \alpha_{N,l} p_{m,k,N}] \quad \forall l, m, k$ and that $\|\mathbf{x}\|_2 \leq \|\mathbf{x}\|_1$, and one can obtain a substitute for C3 as

$$\begin{aligned}
 & \sum_{m \in \mathcal{M}} \sum_{k \in \mathcal{K}_m} \sum_{n \in \Omega_k} \gamma_{n,l} p_{m,k,n} \\
 & + \sqrt{2 \log \frac{1}{\epsilon}} |\sigma_{n,l} \alpha_{n,l} p_{m,k,n}| \leq I_l^{th} \quad \forall l \tag{16}
 \end{aligned}$$

where $\gamma_{n,l} \triangleq \mu_{n,l}^+ \alpha_{n,l} + \beta_{n,l}$.

2) *Centralized Power Allocation for Femtocells*: The power-allocation problem with chance-constrained approximation can be rewritten as

$$\begin{aligned}
& \max_{p_{m,k,n}} \sum_{m \in \mathcal{M}} \sum_{k \in \mathcal{K}_m} \sum_{n \in \Omega_k} r_{m,k,n} \\
\text{s.t. } & \text{C1: } \sum_{n \in \Omega_k} r_{m,k,n} \geq R_{k,\min} \quad \forall m, k \in \mathcal{K}_m \\
& \text{C2: } \sum_{k \in \mathcal{K}_m} \sum_{n \in \Omega_k} p_{m,k,n} \leq P_t \quad \forall m \\
& \text{C3: } \sum_{m \in \mathcal{M}} \sum_{k \in \mathcal{K}_m} \sum_{n \in \Omega_k} \left(\gamma_{n,l} p_{m,k,n} \right. \\
& \quad \left. + \sqrt{2 \log \left(\frac{1}{\epsilon} \right) |\sigma_{n,l} \alpha_{n,l} p_{m,k,n}|} \right) \\
& \leq I_l^{th} \quad \forall l \\
& \text{C4: } p_{m,k,n} \geq 0 \quad \forall m, k, n.
\end{aligned} \tag{17}$$

Equation (17) defines a convex optimization problem and can be solved by barrier method [34]. The logarithmic barrier function is

$$\begin{aligned}
\phi(\mathbf{x}) = & - \sum_{m \in \mathcal{M}} \sum_{k \in \mathcal{K}_m} \log \left(\sum_{n \in \Omega_k} r_{m,k,n} - R_{k,\min} \right) \\
& - \sum_{m \in \mathcal{M}} \log \left(P_t - \sum_{k \in \mathcal{K}_m} \sum_{n \in \Omega_k} p_{m,k,n} \right) \\
& - \sum_{l=1}^L \log \left(I_l^{th} - \sum_{m \in \mathcal{M}} \sum_{k \in \mathcal{K}_m} \sum_{n \in \Omega_k} \left(p_{m,k,n} \gamma_{n,l} \right. \right. \\
& \quad \left. \left. + \sqrt{2 \log \frac{1}{\epsilon} |\sigma_{n,l} \alpha_{n,l} p_{m,k,n}|} \right) \right) \\
& - \sum_{m \in \mathcal{M}} \sum_{k \in \mathcal{K}_m} \sum_{n \in \Omega_k} \log p_{m,k,n}
\end{aligned} \tag{18}$$

where $\mathbf{x} = (p_{m,k,1}, p_{m,k,2}, \dots, p_{m,k,N})$. Note that subscript k can be omitted as it has been determined by subchannel allocation. Denote

$$f(\mathbf{x}) = \sum_{m \in \mathcal{M}} \sum_{k \in \mathcal{K}_m} R_{m,k} \tag{19}$$

where $R_{m,k} = \sum_{n \in \Omega_k} r_{m,k,n}$; the optimal solution to problem (17) can be approximated by solving the following unconstrained minimization problem:

$$\min \psi_t(\mathbf{x}) = -t f(\mathbf{x}) + \phi(\mathbf{x}) \tag{20}$$

where $t \geq 0$ is a parameter to control the accuracy of solution. Newton method can efficiently solve this unconstrained minimization problem.

The Newton step at \mathbf{x} , denoted by $\Delta \mathbf{x}_{nt}$, is given by

$$\nabla^2 \psi_t(\mathbf{x}) \Delta \mathbf{x}_{nt} = -\nabla \psi_t(\mathbf{x}) \tag{21}$$

where $\nabla \psi_t(\mathbf{x})$ and $\nabla^2 \psi_t(\mathbf{x})$ are the gradient and the Hessian of $\psi_t(\mathbf{x})$, respectively.

The procedure of the barrier method is outlined in Table III. ξ and ξ_n are the tolerance values of the barrier method and

TABLE III
BARRIER METHOD

Barrier method	
1	Initialization for Barrier method
2	Find feasible point \mathbf{x} ; Set $t := t^{(0)} > 0$, $\xi > 0$, $\mu > 1$,
3	$\alpha \in (0, 1/2)$, $\beta \in (0, 1)$.
4	Outer Loop for Barrier method
5	Stopping criterion of Barrier method: $(MKN + L)/t < \xi$
6	Initialization for Newton method
7	Tolerance $\xi_n > 0$, $\alpha \in (0, 1/2)$, $\beta \in (0, 1)$;
8	Inner Loop for Newton method
9	Compute $\Delta \mathbf{x}_{nt}$ and $\lambda := -\nabla \psi_t(\mathbf{x}) \Delta \mathbf{x}_{nt}$;
10	Stopping criterion of Newton method: $\lambda^2/2 \leq \xi_n$
11	Backtracking line search on $\psi_t(\mathbf{x})$, $w := 1$;
12	while $\psi_t(\mathbf{x} + w \Delta \mathbf{x}) > \psi_t(\mathbf{x}) - \alpha w \lambda^2$
13	Update: $w := \beta w$
14	endwhile
15	Update: $\mathbf{x} = \mathbf{x} + w \Delta \mathbf{x}$
16	Update: $t := \mu t$

the Newton step, respectively. α and β are two given constants applied in the backtracking line search in the Newton step. In addition, α is set as $\alpha \in (0, 0.5)$, and β is set as $\beta \in (0, 1)$, respectively. The step size of the backtracking line search is s with $s > 0$. t and μ are the parameters used in the tradeoff between the number of the outer and the inner iterations.

The computational complexity of the barrier method mainly lies in the computation of Newton step that needs matrix inversion. To reduce the computational cost, we exploit the structure of (17) and develop a fast algorithm to calculate Newton step with lower complexity. Denote

$$\begin{aligned}
f_m &= P_t - \sum_{k \in \mathcal{K}_m} \sum_{n \in \Omega_k} p_{m,k,n}, \quad m = 1, \dots, M \\
f_{k+M} &= \sum_{n \in \Omega_k} r_{m,k,n} - R_{k,\min}, \quad k = 1, \dots, K \\
g_l &= I_l^{th} - \sum_{m \in \mathcal{M}} \sum_{k \in \mathcal{K}_m} \sum_{n \in \Omega_k} \left(p_{m,k,n} \gamma_{n,l} \right. \\
& \quad \left. + \sqrt{2 \log \frac{1}{\epsilon} |\sigma_{n,l} \alpha_{n,l} p_{m,k,n}|} \right) \\
& \quad l = 1, \dots, L.
\end{aligned} \tag{22}$$

The Hessian of $\psi_t(\mathbf{x})$ is

$$\begin{aligned}
\nabla^2 \psi_t(\mathbf{x}) = & \begin{bmatrix} D_1 & & & \\ & D_2 & & \\ & & \ddots & \\ & & & D_N \end{bmatrix} \\
& + \sum_{m=1}^M \frac{\nabla f_m \nabla f_m^T}{f_m^2} + \sum_{k=1}^K \frac{\nabla f_{k+M} \nabla f_{k+M}^T}{f_{k+M}^2} \\
& + \sum_{l=1}^L \frac{\nabla g_l \nabla g_l^T}{g_l^2} \\
& = D + \sum_{i=1}^S F_i F_i^T
\end{aligned} \tag{23}$$

TABLE IV
SIMULATION PARAMETERS

System Parameters	Radius of Macro-network	500 m (LTE-A)
	Carrier Frequency	2 GHz
	Total Bandwidth	100 MHz
	Thermal Noise PSD	-174 dBm/Hz
	Parameter ϵ	0.1
Shadowing	Shadow Fading	Log-normal
Macrocell Parameters	Transmit Power	46 dBm
	Antenna Gain	14 dBi
	Noise Figure	7 dB
Femtocell Parameters	Transmit Power	23 dBm
	Noise Figure	7 dB
M(F)U Parameters	Antenna Gain	0 dBi
	Noise Figure	7dB

where $D = \text{diag}(D_1, D_2, \dots, D_N)$, and $S = M + K + L$ with

$$D_n = \left(t + \frac{1}{f_k} \right) \frac{H_{m,k,n}^2}{(1 + p_{m,k,n} H_{m,k,n})^2} + \frac{1}{p_{m,k,n}^2}. \quad (24)$$

F_i are all vectors with N elements

$$F_i = \begin{cases} \frac{\nabla f_m}{f_m}, & m = 1, \dots, M, i = m \\ \frac{\nabla f_{k+M}}{f_{k+M}}, & k = 1, \dots, K, i = k + M \\ \frac{\nabla g_l}{g_l}, & l = 1, \dots, L, i = l + M + K. \end{cases} \quad (25)$$

Theorem 1: Equation (17) can be solved with the complexity of $O(S^2N)$.

The proof is given in the Appendix. If we solve (17) via a standard convex optimization technique, it yields a complexity of $O(N^3)$. In practical wireless systems, $S \ll N$ and our proposed algorithm have a significant advantage.

IV. NUMERICAL RESULTS AND DISCUSSIONS

Consider the downlink of an LTE-Advanced (LTE-A) network in which a macrocell is in the center of a circle with a radius of 500 m. In addition, the two femtocells with four FUs are within the coverage of the macrocell. A dual-stripe building model, which was initially proposed in [35], is adopted to evaluate the performance of our algorithm. The channel gains between the macrocell and the FUs are modeled as independent and identically distributed (i.i.d.) and exponentially distributed with $\bar{g}_{k,n} = 2$ for all k and n . Parameters $\mu_n^+ = \mu_n^-$ and σ_n in the Bernstein approximations are chosen from Table I in [33] using the known first- and second-order moments of the truncated channel gains. The simulation parameters are listed in Table IV.

The distance-dependent path-loss attenuation varies according to the characteristics of the evaluated link. We give a summary of the different situations adopted in [35] in our simulations.

- Macrocell to MU/FU

$$PL(d) = 15.3 + 37.6 \log_{10}(d) + L_{ow}. \quad (26)$$

We use a simplified version of the Motley–Keenan model to characterize the path loss attenuation in this case,

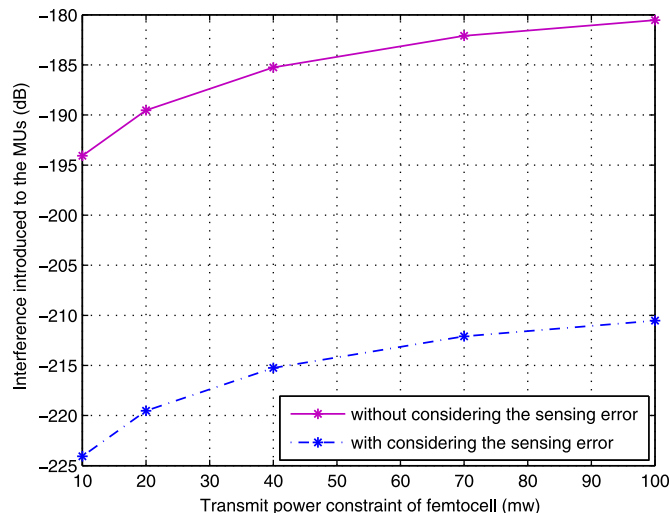


Fig. 2. Interference to the MUs as a function of transmission power limit.

where d is the distance between the macrocell and the MU/FU, and L_{ow} is the penetration loss in the external walls of the building, which is 10 dB.

- Femtocell to FU/MU

$$PL(d) = 38.46 + 20 \log_{10}(d) + 0.7d_{2D} + qL_{iw} + 18.3n^{\left(\frac{n+2}{n+1} - 0.46\right)} \quad (27)$$

where d is the distance between the femtocell and the FU; d_{2D} is the indoor distance of the link; L_{iw} is the penetration loss in the internal walls of the building, which is 5 dB; and $q(n)$ denotes the number of penetrated walls (floors).

Shadow fading is modeled as a log-normal random variable, whose standard deviation is 4 and 8 dB for the MUs and the FUs, respectively. About fast fading, in the frequency domain, the channel gains for subchannels are modeled as i.i.d. zero-mean circularly symmetric complex Gaussian random variables. The activity probability P_n^L , misdetection P_n^m , and false alarm P_n^f are uniformly distributed over (0, 1), (0.01, 0.05), and (0.05, 0.1), respectively.

Fig. 2 shows the interference to the MUs with and without considering the sensing errors. As shown in Fig. 2, the interference introduced to the MUs with considering the sensing errors is lower than the interference without considering the sensing errors. It can be explained that the MUs may experience severe performance degradation when the cross-tier interference occurs as a result of misdetection.

We also make a comparison between our proposed optimal power-allocation algorithm with other two algorithms to evaluate the sum capacity performance, namely, equal power-allocation (EPA) algorithm and interference-factor power-allocation (IFPA) algorithm. The former assumes that power is equally allocated among all subchannels, and the latter assumes that the distributed power is inversely proportional to the interference level.

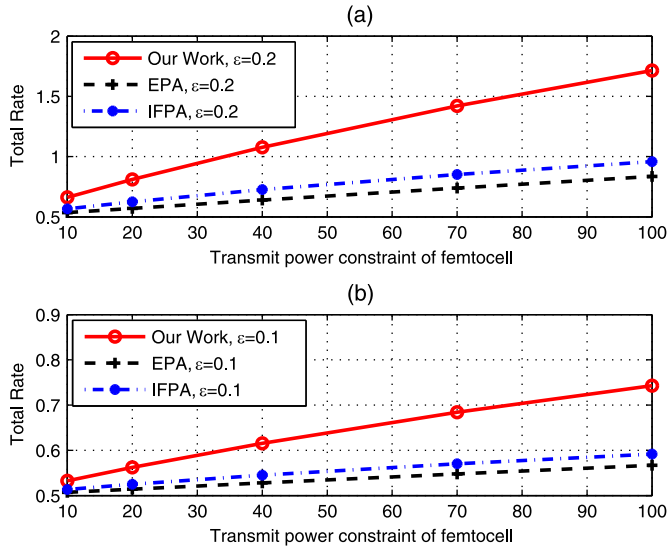


Fig. 3. Sum capacity as a function of transmission power limit. (a) $\epsilon = 0.2$. (b) $\epsilon = 0.1$.

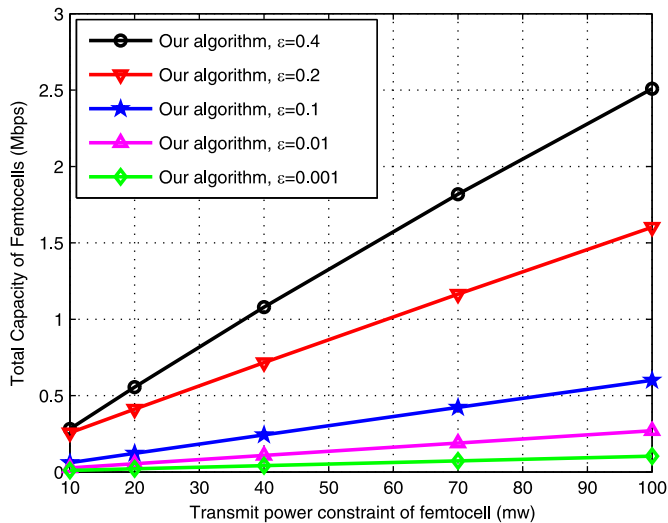


Fig. 4. Sum capacity versus ϵ .

Fig. 3 shows the sum capacity of the femtocells as a function of power limit achieved by our proposed algorithm, EPA algorithm, and IFPA algorithm. There are 256 subchannels. In Fig. 3, we can see that the sum capacity of the FUs grows as the increase in the power budget. Our proposed algorithm performs better than the EPA and the IFPA. When power budget is small, the IFPA can produce solutions close to our proposed schemes. However, when power budget grows larger, our algorithm performs much better than the others. This is because our proposed subchannel allocation schemes jointly consider the power limit and interference level, but the EPA and the IFPA only consider one of them.

We validate the effect of ϵ in sum capacity. As shown in Fig. 4, the sum capacity of the FUs grows with the increase in ϵ . It is intuitive because smaller ϵ tightens the interference constraints, which introduces lower interference to the MUs. Our proposed algorithm jointly considers the interference

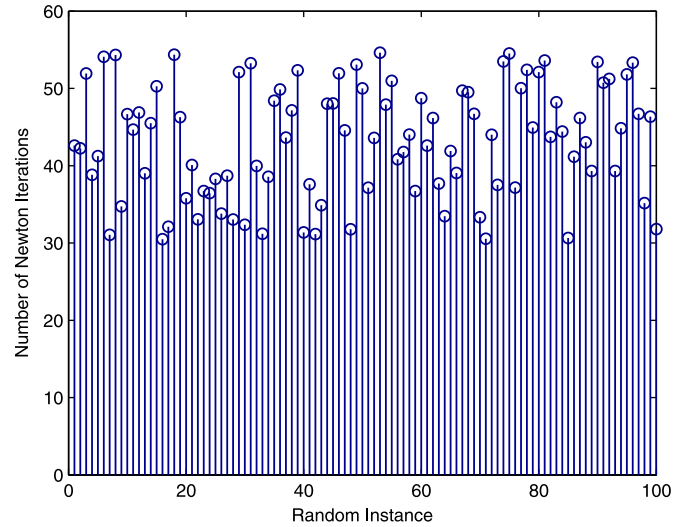


Fig. 5. Number of Newton iterations required for convergence during 100 channel realizations.

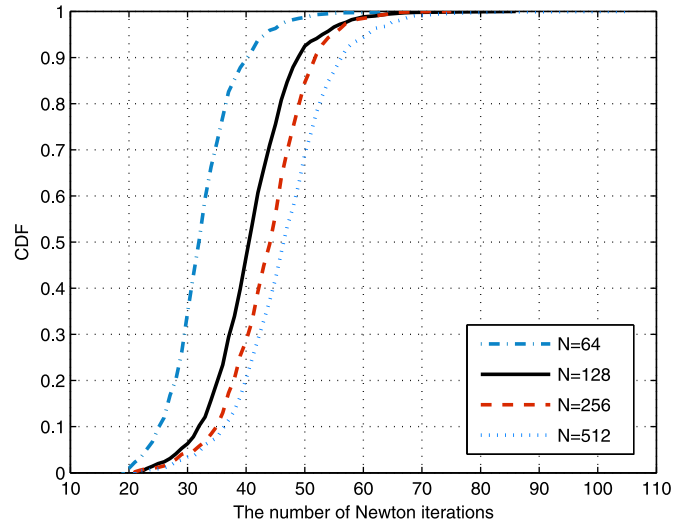


Fig. 6. Empirical CDF of the number of Newton iterations.

introduced to the MUs and the SNR of subchannels; lower interference is achieved at the cost of capacity reduction, as shown in Fig. 4.

We also investigate the convergence of our proposed fast algorithm. As previously discussed, the computational load of the proposed algorithm mainly lies in the computation of Newton step. Fig. 5 shows the number of Newton iterations for the barrier method to converge in 100 random instances. Fig. 6 gives the cumulative distribution function (CDF) of the number of Newton iterations for solving the optimal power allocation with different settings of the number of N . As shown in Fig. 6, the number of Newton iterations is not large and varies in a narrow range, indicating that our proposed algorithm is efficient.

Finally, we investigate the densely deployed femtocells' case and take the intratier interference among femtocells into consideration. Mathematically, the intratier interference should be added into the denominator of (5). In addition, similar to

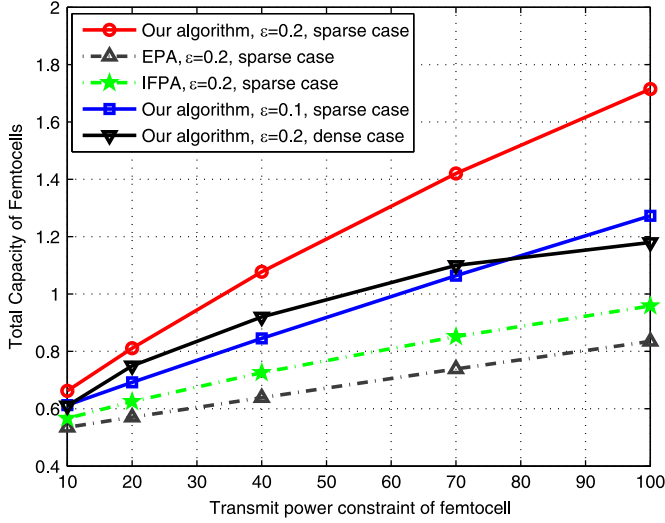


Fig. 7. Total downlink capacity of all femtocells as a function of transmit power limit.

C3 in (7), an intratier interference temperature constraint I_{th}^m should be introduced; by our proposed subchannel allocation, the corresponding nonconvex subchannel and power-allocation problem can be converted into a convex problem. Fig. 7 shows the overall capacity of M femtocells in the cases of sparsely deployed scenarios and densely deployed scenarios. We set $M = 40$, $K = 4$, and $I_{th}^m = 7.5 \times 10^{-14}$ W for all m . We can see that, in Fig. 7, the total capacity of the femtocells in dense deployment situation is smaller than that of the sparsely deployed case. The reason is that there exists heavy intratier interference among femtocells, which counteracts the capacity yielded by adding femtocells.

V. CONCLUSION

In this paper, we have developed a fast algorithm for the RA problem in a CR-based femtocell network with channel uncertainty and imperfect spectrum sensing, which is an extension of our preliminary research [36]. In particular, the sum rate of all FUs is maximized while the interference to each MU is kept below a threshold. The formulated optimization task involves integer variables and chance constraints, making it hard to address. We first develop an efficient subchannel allocation to remove the frustrating integer constraints. Then, we introduce Bernstein approximation to make chance constraints tractable. Finally, we derive a fast barrier method to work out the optimal power distribution by updating Newton step with almost linear complexity. Numerical simulations show that our proposed RA method can achieve a significant capacity gain, and our proposed algorithm converges quickly and stably.

APPENDIX

Proof: Rewrite the Karush–Kuhn–Tucker system (21) as follows:

$$\Lambda_0 \Delta \mathbf{x} = F_0 \quad (28)$$

where $\Lambda_0 = \nabla^2 \psi_t$, and $F_0 = -\nabla \psi_t$. According to (23), Λ_0 can be written as

$$\Lambda_0 = D + \sum_{i=1}^S F_i F_i^T \quad (29)$$

which can be decomposed into S equations

$$\Lambda_i = \Lambda_{i+1} + F_{i+1} F_{i+1}^T, i = 0, 1, \dots, S - 1. \quad (30)$$

By exploiting the structure of Λ_i 's, we give an S -step procedure to compute Newton step efficiently.

First, use (30) to decompose Λ_0 , i.e., $\Lambda_0 = \Lambda_1 + F_1 F_1^T$. Denote two intermediate variables as the solutions of the following linear equations: $\Lambda_1 v_1^1 = F_0$ and $\Lambda_1 v_2^1 = F_1$. $\Delta \mathbf{x} = v_1^1 - (F_1 v_1^1 / 1 + F_1 v_2^1) v_2^1$. In addition, we can figure out $\Delta \mathbf{x}$ if obtaining the two new variables v_1^1 and v_2^1 .

Continuing the procedure, decompose Λ_1 with $\Lambda_1 = \Lambda_2 + F_2 F_2^T$. Then, the two variables introduced in step 1 can be updated by solving the following three sets of linear equations: $\Lambda_2 v_i^2 = F_{i-1}$, $i = 1, 2, 3$, where v_1^2 , v_2^2 and v_3^2 are intermediate variables.

For the s th step, decompose Λ_{s-1} with $\Lambda_s = \Lambda_s + F_s F_s^T$. We can update the s variables introduced in step $s - 1$ by $v_i^{s-1} = v_i^s - (F_s^T v_i^s / 1 + F_s v_{s+1}^s) v_{s+1}^s$, $i = 1, 2, \dots, s$, which is obtained by solving the following $s + 1$ sets of linear equations: $\Lambda_s v_i^s = F_{i-1}$, $i = 1, 2, \dots, s + 1$.

Continuing the procedure to the S th step, it yields $S + 1$ matrix systems $\Lambda_S v_i^S = F_{i-1}$, $i = 1, 2, \dots, S + 1$. From the derivation process, we can find that the m variables v_i^{s-1} , $i = 1, 2, \dots, s$ in the $(s - 1)$ th step can be obtained by the $s + 1$ variables v_i^s , $i = 1, 2, \dots, s + 1$ in the s th step. Thus, if we figure out the $S + 1$ variables v_i^S , $i = 1, 2, \dots, S + 1$, $\Delta \mathbf{x}$ will be indirectly obtained. Obviously, a reverse derivation of the S steps is necessary after we solve the $S + 1$ matrix system in the S th step.

The process to solve the matrix equation $\Lambda_S v_i^S = F_{i-1}$ is as follows: According to the analysis given in Section IV, we have $\Lambda_S = D$. Unify these equations into

$$\begin{bmatrix} D_1 & & & & \\ & D_2 & & & \\ & & \ddots & & \\ & & & \ddots & \\ & & & & D_N \end{bmatrix} v = g. \quad (31)$$

Since D is a diagonal matrix, we can easily obtain

$$v_i = D_i^{-1} g_i, i = 1, \dots, N. \quad (32)$$

Thus, the computational complexity of solving the $S + 1$ matrix systems is $O(SN)$. We also need an S -step reverse iteration to figure out $\Delta \mathbf{x}$. The total computational cost for the proposed method is $O(S^2 N)$. ■

ACKNOWLEDGMENT

The authors would like to thank the editors and the anonymous reviewers whose invaluable comments helped improve the presentation of this paper substantially.

REFERENCES

- [1] D. Lopez-Perez, A. Valcarce, G. de la Roche, and J. Zhang, "OFDMA femtocells: A roadmap on interference avoidance," *IEEE Commun. Mag.*, vol. 47, no. 9, pp. 41–48, Sep. 2009.
- [2] V. Chandrasekhar, J. Andrews, and A. Gatherer, "Femtocell networks: A survey," *IEEE Commun. Mag.*, vol. 46, no. 9, pp. 59–67, Sep. 2008.
- [3] J.-H. Yun and K. Shin, "Adaptive interference management of OFDMA femtocells for co-channel deployment," *IEEE J. Sel. Areas Commun.*, vol. 29, no. 6, pp. 1225–1241, Jun. 2011.
- [4] D. Lopez-Perez *et al.*, "Enhanced intercell interference coordination challenges in heterogeneous networks," *IEEE Wireless Commun. Mag.*, vol. 18, no. 3, pp. 22–30, Jun. 2011.
- [5] V. Chandrasekhar, J. Andrews, T. Muharemovict, Z. Shen, and A. Gatherer, "Power control in two-tier femtocell networks," *IEEE Trans. Wireless Commun.*, vol. 8, no. 8, pp. 4316–4328, Aug. 2009.
- [6] H. Wang and Z. Ding, "Macrocell-queue-stabilization-based power control of femtocell networks," *IEEE Trans. Wireless Commun.*, vol. 13, no. 9, pp. 5223–5236, Sep. 2014.
- [7] T. M. Nguyen, Y. Jeong, T. Quek, W. P. Tay, and H. Shin, "Interference alignment in a Poisson field of MIMO femtocells," *IEEE Trans. Wireless Commun.*, vol. 12, no. 6, pp. 2633–2645, Jun. 2013.
- [8] I. Guvenc, M.-R. Jeong, F. Watanabe, and H. Inamura, "A hybrid frequency assignment for femtocells and coverage area analysis for co-channel operation," *IEEE Commun. Lett.*, vol. 12, no. 12, pp. 880–882, Dec. 2008.
- [9] V. Chandrasekhar and J. Andrews, "Spectrum allocation in tiered cellular networks," *IEEE Trans. Commun.*, vol. 57, no. 10, pp. 3059–3068, Oct. 2009.
- [10] W. C. Cheung, T. Quek, and M. Kountouris, "Throughput optimization, spectrum allocation, and access control in two-tier femtocell networks," *IEEE J. Sel. Areas Commun.*, vol. 30, no. 3, pp. 561–574, Apr. 2012.
- [11] H. Zhang *et al.*, "Resource allocation in spectrum-sharing OFDMA femtocells with heterogeneous services," *IEEE Trans. Commun.*, vol. 62, no. 7, pp. 2366–2377, Jul. 2014.
- [12] X. Ge *et al.*, "Spectrum and energy efficiency evaluation of two-tier femtocell networks with partially open channels," *IEEE Trans. Veh. Technol.*, vol. 63, no. 3, pp. 1306–1319, Mar. 2014.
- [13] D.-C. Oh, H.-C. Lee, and Y.-H. Lee, "Power control and beamforming for femtocells in the presence of channel uncertainty," *IEEE Trans. Veh. Technol.*, vol. 60, no. 6, pp. 2545–2554, Jul. 2011.
- [14] S. Guruacharya, D. Niyato, D. I. Kim, and E. Hossain, "Hierarchical competition for downlink power allocation in OFDMA femtocell networks," *IEEE Trans. Wireless Commun.*, vol. 12, no. 4, pp. 1543–1553, Apr. 2013.
- [15] H. Kpojime and G. Safdar, "Interference mitigation in cognitive radio based femtocells," *IEEE Commun. Surveys Tuts.*, vol. 17, no. 3, pp. 1511–1534, 3rd Quart. 2015.
- [16] N. Saquib, E. Hossain, L. B. Le, and D. I. Kim, "Interference management in OFDMA femtocell networks: Issues and approaches," *IEEE Wireless Commun.*, vol. 19, no. 3, pp. 86–95, Jun. 2012.
- [17] X. Chu, Y. Wu, D. Lopez-Perez, and X. Tao, "On providing downlink services in collocated spectrum-sharing macro and femto networks," *IEEE Trans. Wireless Commun.*, vol. 10, no. 12, pp. 4306–4315, Dec. 2011.
- [18] S.-M. Cheng, W. C. Ao, F.-M. Tseng, and K.-C. Chen, "Design and analysis of downlink spectrum sharing in two-tier cognitive femto networks," *IEEE Trans. Veh. Technol.*, vol. 61, no. 5, pp. 2194–2207, Jun. 2012.
- [19] L. Li, C. Xu, and M. Tao, "Resource allocation in open access OFDMA femtocell networks," *IEEE Wireless Commun. Lett.*, vol. 1, no. 6, pp. 625–628, Dec. 2012.
- [20] J. Huang and V. Krishnamurthy, "Cognitive base stations in LTE/3GPP femtocells: A correlated equilibrium game-theoretic approach," *IEEE Trans. Commun.*, vol. 59, no. 12, pp. 3485–3493, Dec. 2011.
- [21] R. Urgaonkar and M. Neely, "Opportunistic cooperation in cognitive femtocell networks," *IEEE J. Sel. Areas Commun.*, vol. 30, no. 3, pp. 607–616, Apr. 2012.
- [22] Z. Liu, J. Wang, Y. Xia, and H. Yang, "Robust optimisation of power control for femtocell networks," *IET Signal Process.*, vol. 7, no. 5, pp. 360–367, Jul. 2013.
- [23] K.-Y. Wang, N. Jacklin, Z. Ding, and C.-Y. Chi, "Robust MISO transmit optimization under outage-based QoS constraints in two-tier heterogeneous networks," *IEEE Trans. Wireless Commun.*, vol. 12, no. 4, pp. 1883–1897, Apr. 2013.
- [24] L. Zhou, Z. Yang, Y. Wen, H. Wang, and M. Guizani, "Resource allocation with incomplete information for QoE-driven multimedia communications," *IEEE Trans. Wireless Commun.*, vol. 12, no. 8, pp. 3733–3745, Aug. 2013.
- [25] L. Zhou, Z. Yang, Y. Wen, and J. Rodrigues, "Distributed wireless video scheduling with delayed control information," *IEEE Trans. Circuits Syst. Video Technol.*, vol. 24, no. 5, pp. 889–901, May 2014.
- [26] N. Y. Soltani, S.-J. Kim, and G. B. Giannakis, "Chance-constrained optimization of OFDMA cognitive radio uplinks," *IEEE Trans. Wireless Commun.*, vol. 12, no. 3, pp. 1098–1107, Mar. 2013.
- [27] S. Wang, Z.-H. Zhou, M. Ge, and C. Wang, "Resource allocation for heterogeneous cognitive radio networks with imperfect spectrum sensing," *IEEE J. Sel. Areas Commun.*, vol. 31, no. 3, pp. 464–475, Mar. 2013.
- [28] S. Wang, Z.-H. Zhou, M. Ge, and C. Wang, "Resource allocation for heterogeneous multiuser OFDM-based cognitive radio networks with imperfect spectrum sensing," in *Proc. IEEE INFOCOM*, Mar. 2012, pp. 2264–2272.
- [29] A. Goldsmith and S.-G. Chua, "Variable-rate variable-power MQAM for fading channels," *IEEE Trans. Commun.*, vol. 45, no. 10, pp. 1218–1230, Oct. 1997.
- [30] S. Wang, "Efficient resource allocation algorithm for cognitive OFDM systems," *IEEE Commun. Lett.*, vol. 14, no. 8, pp. 725–727, Aug. 2010.
- [31] S. Wang, M. Ge, and C. Wang, "Efficient resource allocation for cognitive radio networks with cooperative relays," *IEEE J. Sel. Areas Commun.*, vol. 31, no. 11, pp. 2432–2441, Nov. 2013.
- [32] A. Nemirovski and A. Shapiro, "Convex approximations of chance constrained programs," *SIAM J. Optim.*, vol. 17, no. 4, pp. 969–996, May 2006.
- [33] A. Ben-Tal and A. Nemirovski, "Selected topics in robust convex optimization," *Math. Program.*, vol. 112, no. 1, pp. 125–158, Mar. 2008.
- [34] S. Boyd and L. Vandenberghe, *Convex Optimization*. Cambridge, U.K.: Cambridge Univ. Press, 2004.
- [35] "Simulation assumptions and parameters for FDD HeNB RF requirements," Third-Generation Partnership Project, Sophia Antipolis Cedex, France, R4-092042, TSG-RAN WG4, Meet. 51, 2009.
- [36] Y. Zhang and S. Wang, "Resource allocation for femtocell networks by using chance-constrained optimization," in *Proc. IEEE WCNC*, Mar. 2015, pp. 1805–1810.



Yujie Zhang received the B.S. degree in communication engineering in 2013 from Nanjing University, Nanjing, China, where she is currently working toward the M.S. degree with the School of Electronic Science and Engineering.

Her research interests include wireless communications and convex optimization. Currently, her research focuses on resource allocation in heterogeneous cellular networks.



Shaowei Wang (S'06–M'07–SM'13) received the B.S., M.S., and Ph.D. degrees from Wuhan University, Wuhan, China, in 1997, 2003, and 2006, respectively, all in electronic engineering.

From 1997 to 2001, he was an R&D Scientist with China Telecom. Since 2006, he has been with the School of Electronic Science and Engineering, Nanjing University, Nanjing, China. From 2012 to 2013, he was a Visiting Scholar/Professor with Stanford University, Stanford, CA, USA, and with The University of British Columbia, Vancouver, BC, Canada. He has published more than 70 papers in leading journals and conference proceedings in his areas of interest.

Dr. Wang organized the Special Issue on Enhancing Spectral Efficiency for LTE-Advanced and Beyond Cellular Networks for *IEEE Wireless Communications* and the Feature Topic on Energy-Efficient Cognitive Radio Networks for *IEEE Communications Magazine*. He is with the editorial board of *IEEE Communications Magazine* and the IEEE TRANSACTIONS ON WIRELESS COMMUNICATIONS. He serves/served on the technical or executive committee of several reputable conferences, including the IEEE International Conference on Computer Communications (INFOCOM), the IEEE International Conference on Communications (ICC), the IEEE Global Communications Conference (GLOBECOM), the IEEE Wireless Communications and Networking Conference (WCNC), etc.